JACS
JOURNAL OF THE AMERICAN CHEMICAL SOCIETY
Article
pubs.acs.org/JACS

Discovery and Biosynthesis of Gladiolin: A *Burkholderia gladioli* Antibiotic with Promising Activity against *Mycobacterium tuberculosis*

Lijiang Song,[†,∥] Matthew Jenner,[†,∥] Joleen Masschelein,[†,∥] Cerith Jones,[‡] Matthew J. Bull,[‡] Simon R. Harris,[§] Ruben C. Hartkoorn,[⊥] Anthony Vocat,[⊥] Isolda Romero-Canelon,[†] Paul Coupland,[‡] Gordon Webster,[‡] Matthew Dunn,[§] Rebecca Weiser,[‡] Christopher Paisey,[‡] Stewart T. Cole,[⊥] Julian Parkhill,[§] Eshwar Mahenthiralingam,[*,‡] and Gregory L. Challis[*,‡]

[†]Department of Chemistry, University of Warwick, Coventry CV4 7AL, United Kingdom
[‡]Organisms and Environment Research Division, Cardiff School of Biosciences, Cardiff University, Cardiff CF10 3AT, United Kingdom
[§]Wellcome Trust Sanger Institute, Wellcome Trust Genome Campus, Hinxton, Cambridge CB10 1SA, United Kingdom
[⊥]Global Health Institute, Ecole Polytechnique Fédérale de Lausanne, Station 19, 1015 Lausanne, Switzerland

Supporting Information

ABSTRACT: An antimicrobial activity screen of *Burkholderia gladioli* BCC0238, a clinical isolate from a cystic fibrosis patient, led to the discovery of gladiolin, a novel macrolide antibiotic with potent activity against *Mycobacterium tuberculosis* H37Rv. Gladiolin is structurally related to etnangien, a highly unstable antibiotic from *Sorangium cellulosum* that is also active against Mycobacteria. Like etnangien, gladiolin was found to inhibit RNA polymerase, a validated drug target in *M. tuberculosis*. However, gladiolin lacks the highly labile hexaene moiety of etnangien and was thus found to possess significantly increased chemical stability. Moreover, gladiolin displayed low mammalian cytotoxicity and good activity against several *M. tuberculosis* clinical isolates, including four that are resistant to isoniazid and one that is resistant to both isoniazid and rifampicin. Overall, these data suggest that gladiolin may represent a useful starting point for the development of novel drugs to tackle multidrug-resistant tuberculosis. The *B. gladioli* BCC0238 genome was sequenced using Single Molecule Real Time (SMRT) technology. This resulted in four contiguous sequences: two large circular chromosomes and two smaller putative plasmids. Analysis of the chromosome sequences identified 49 putative specialized metabolite biosynthetic gene clusters. One such gene cluster, located on the smaller of the two chromosomes, encodes a *trans*-acyltransferase (*trans*-AT) polyketide synthase (PKS) multienzyme that was hypothesized to assemble gladiolin. Insertional inactivation of a gene in this cluster encoding one of the PKS subunits abrogated gladiolin production, confirming that the gene cluster is responsible for biosynthesis of the antibiotic. Comparison of the PKSs responsible for the assembly of gladiolin and etnangien showed that they possess a remarkably similar architecture, obfuscating the biosynthetic mechanisms responsible for most of the structural differences between the two metabolites.

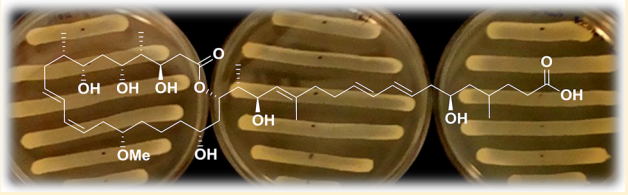

INTRODUCTION

The genus *Burkholderia* comprises a highly diverse group of Gram-negative bacteria that is able to thrive in different ecological niches, ranging from the plant rhizosphere to the human lung.[1] Much of this versatility can be attributed to their relatively large (6 to 9 Mb) GC-rich multireplicon genomes that have evolved to mediate a variety of beneficial and antagonistic interactions with other pro- and eukaryotic organisms.[2] Indeed, *Burkholderia* species are well-known for their ability to promote plant growth, degrade polyaromatic hydrocarbon pollutants, and cause infections in the airways of cystic fibrosis (CF) patients.[3−5] Furthermore, secretion of antimicrobial and other bioactive compounds enables these bacteria to suppress plant pathogenic fungi and nematodes, cause plant diseases, and eliminate other bacterial competitors in their native habitat.[4,6,7] Several studies have demonstrated that *Burkholderia* species are prolific producers of bioactive specialized metabolites, many of which are assembled by *trans*-acyltransferase (AT) polyketide synthase (PKS) or hybrid *trans*-AT PKS-nonribosomal peptide synthetase (NRPS) biosynthetic assembly lines.[8,9] Prominent examples include the following: the phytotoxin rhizoxin;[10] the respiratory toxin bongkrekic acid;[11] the thailanstatin,[12] burkholdac,[13] spliceostatin,[14] and thailandamide[15] families of antiproliferative agents; the bactobolin antibiotics;[16] and enacyloxin IIa, an unusual antibiotic from *Burkholderia ambifaria* with clinically relevant activity against multidrug-resistant Gram-negative pathogens

Received: April 4, 2017
Published: May 22, 2017

DOI: 10.1021/jacs.7b03382
J. Am. Chem. Soc. 2017, 139, 7974−7981

such as *Acinetobacter baumannii*.[17] Furthermore, bioinformatics analyses of sequenced *Burkholderia* genomes have revealed a vast untapped potential for specialized metabolite production,[18] which makes this genus a promising resource for discovery of novel bioactive natural products with potential applications in medicine and agriculture.

In an effort to identify novel bioactive metabolites from *Burkholderia*, we set out to explore the potential of the CF isolate *Burkholderia gladioli* BCC0238 to produce antimicrobial compounds. This led to the discovery of gladiolin, a novel macrolide antibiotic with promising activity against *Mycobacterium tuberculosis*. Gladiolin is structurally related to the highly unstable myxobacterial RNA polymerase inhibitor etnangien.[19,20] However, the structural differences between etnangien and gladiolin confer significantly improved chemical stability on the latter.

The genome of *B. gladioli* BCC0238 was sequenced using single-molecule real-time (SMRT) sequencing technology. This revealed a 130 kb gene cluster encoding a *trans*-acyltransferase (AT) PKS that differs from the corresponding multienzyme responsible for etnangien assembly by the substitution of only a single enzymatic domain. Targeted mutagenesis coupled with comparative metabolite profiling confirmed that this gene cluster directs gladiolin biosynthesis. Sequence analysis of the proteins encoded by genes within the cluster allowed a plausible pathway for the assembly of gladiolin to be proposed, raising intriguing questions about the biosynthetic mechanisms underlying the structural differences between etnangien and gladiolin.

RESULTS AND DISCUSSION

Antimicrobial Activity of *B. gladioli* BCC0238. During a screen of *Burkholderia* sp. for the production of bioactive specialized metabolites,[17] *B. gladioli* BCC0238 (LMG-P 26202), isolated in 1996 from the sputum of a child with cystic fibrosis resident in Minneapolis, Minnesota, USA, was found to exhibit broad spectrum antimicrobial activity. Growth of the strain on a solid minimal medium containing glycerol as a sole carbon source[17] and screening using a conventional microbial overlay assay identified antagonism toward Gram-positive bacteria such as methicillin-resistant *Staphylococcus aureus* (MRSA), *Enterococcus faecium* and *Bacillus subtilis*, Gram-negative bacteria such as *Ralstonia mannitolilytica* and *Burkholderia multivorans*, and clinically problematic yeasts including *Candida albicans* (Figure 1).

Purification and Structure Elucidation of Gladiolin. To identify the antimicrobial metabolite(s) produced by *B. gladioli* BCC0238, large-scale cultures of the strain were grown on the solid minimal medium and acetonitrile extracts of the agar were fractionated by semipreparative HPLC. Positive ion mode HR-ESI-Q-TOF-MS analysis of a bioactive fraction with an absorption maximum at 240 nm identified a compound we named gladiolin with the molecular formula $C_{44}H_{74}O_{11}$ (calculated for $C_{44}H_{75}O_{11}^{+}$: 779.5304, found: 779.5309; calculated for $C_{44}H_{74}O_{11}Na^{+}$: 801.5123, found: 801.5124) (Figure S1). This molecular formula was further confirmed by negative ion mode analysis (calculated for $C_{44}H_{73}O_{11}^{-}$: 777.5158, found: 777.5154) (Figure S2). Fragment ions resulting from the neutral loss of CO_2 (44 Da) and two molecules of water (2 × 18 Da) were observed in negative ion mode MS/MS analysis of gladiolin (Figure S3), indicating the presence of a free carboxyl group and two or more hydroxyl groups.

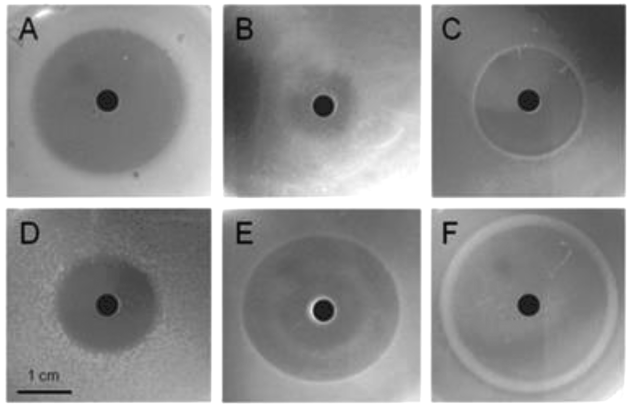

Figure 1. Antimicrobial activity of *B. gladioli* BCC0238. The production of antimicrobial metabolites was screened with a colony overlay assay using (A) methicillin-resistant *S. aureus*, (B) *B. multivorans*, (C) *B. subtilis*, (D) *R. mannitolilytica*, (E) *E. faecium*, and (F) *C. albicans* as indicator strains.

The planar structure of gladiolin was elucidated using a combination of ^{1}H, ^{13}C, COSY, TOCSY, HSQC, HMBC, and NOESY NMR experiments (Figure 2, Tables S1 and S2, Figures S4–S8). Four doublets between 0.69 and 0.80 ppm in the ^{1}H NMR spectrum, each integrating for three protons, indicated that the compound contains four methyl groups attached to methine carbons (Table S1). Singlets at 1.59 and 3.23 ppm, each integrating for three protons, suggested the presence of allylic methyl and methoxy groups, respectively, and several signals between 3.54 and 3.98 ppm and 5.06 and 6.29 ppm indicated that the molecule contains multiple C-hydroxyl groups and carbon–carbon double bonds (Table S1). An unbroken network of COSY correlations established the

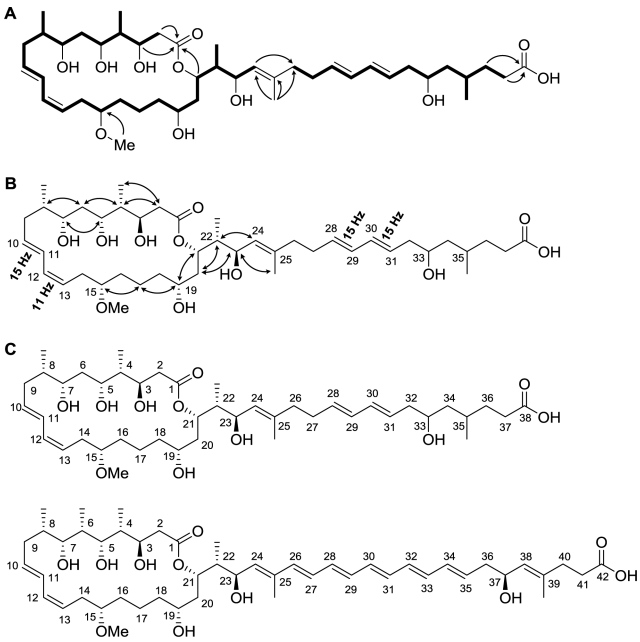

Figure 2. Structure elucidation of gladiolin and comparison with the structure of etnangien. (A) COSY (bold lines) and key HMBC correlations (arrows) observed for gladiolin. (B) Key NOESY correlations and $^{3}J_{H,H}$ coupling constants used to assign the relative stereochemistry of gladiolin. (C) Comparison of the structures of gladiolin (top) and etnangien (bottom).

DOI: 10.1021/jacs.7b03382
J. Am. Chem. Soc. 2017, 139, 7974–7981

structures of the C-2 to C-24 and C-26 to C-37 fragments of the molecule (Figure 2A). HMBC correlations between the protons of the C-25 methyl group and C-24, C-25, and C-26, and between the proton attached to C-24 and C-26, allowed the connectivity of the C-2/C-24 and C-26/C-37 fragments to be determined (Figure 2A). Similarly, the location of the methoxy group was established on the basis of an HMBC correlation between the protons attached to the methyl group and C-15 (Figure 2A). Signals at 174.9 and 170.9 ppm in the ^{13}C NMR spectrum showed that gladiolin contains two carbonyl groups (Table S1). On the basis of HMBC correlations between C-38 and the protons attached to C-36/C-37, and between C-1 and the protons attached to C-2, C-3 and C-21, the former is assigned to a carboxyl group attached to C-37, whereas the latter is assigned to an ester linkage between C-2 and the C-21 hydroxyl group (Figure 2A). The configurations of the double bonds in gladiolin were deduced from NOESY correlations and ^{1}H NMR coupling constants. $^{3}J_{H,H}$ coupling constants of 15 Hz for H-10/H-11, H-28/H-29, and H-30/H-31 and NOESY correlations between the C-25 methyl group and H-23 indicated that the C-10/C-11, C-24/C-25, C-28/C-29 and C-30/C-31 double bonds all have the *E* configuration, whereas a coupling constant of 11 Hz for H-12/H-13 is consistent with a *Z* configuration for the C-12/C-13 double bond (Figure 2B and Table S1).

Gladiolin is structurally related to etnangien, a highly unstable antibiotic produced by *Sorangium cellulosum* (Figure 2C and Figure S9).[19,20] Compared to gladiolin, etnangien has an extra methyl group at C-46, contains four additional unsaturated carbon atoms between C-31 and C-36, and has double bonds in place of single bonds between C-26/C-27 and the carbon atoms C-38/C-39 (corresponding to C-34/C-35 of gladiolin). The instability of etnangien is attributed to its conjugated acyclic hexaene moiety, which is prone to light-induced isomerization and rapid oxidative degradation, necessitating the exclusion of light and the inclusion of the antioxidant 4-*tert*-butylcatechol in all purification steps.[20] No such precautions are necessary during the purification of gladiolin, because it lacks the highly labile hexaene moiety of etnangien and as a consequence is comparatively stable. However, during the course of our studies on the structure of gladiolin we found that it undergoes slow conversion (approximately 75% after 96 h at room temperature) to an isomer upon standing in methanol (Figure S10). Structure elucidation of this isomer using 1- and 2-D NMR spectroscopy showed that it results from nucleophilic addition of the C-23 hydroxyl group to the ester, followed by elimination of the C-21 hydroxyl group to form a 24-membered lactone (Figure S11, Table S3). The rate of this rearrangement was found to be much slower in 9:1 H_20/DMSO (20% after 65 days at room temperature), suggesting that it is unlikely to pose problems in relation to potential therapeutic applications of gladiolin.

NOESY NMR data for gladiolin indicate that the C-3 to C-23 segment of gladiolin has the same relative stereochemistry as the corresponding portion of etnangien (Figure 2C and S9).[21] Moreover, this agrees with the relative and absolute stereochemistry deduced for gladiolin on the basis of predictive sequence analysis of ketoreductase (KR) domain stereospecificity within the gladiolin polyketide synthase (see the section on gladiolin biosynthesis below). The absolute configuration of C-33 can similarly be predicted on the basis of the KR stereospecificity analysis, but the configuration of C-35 remains unknown and requires further experimental investigation.

Antimicrobial Activity and Cytotoxicity of Gladiolin. Purified gladiolin was tested for its antimicrobial activity against a range of Gram-positive and Gram-negative bacteria, including representative members of the ESKAPE panel of pathogens.[22] Moderate activity was observed against Gram-positive bacteria such as MRSA and *E. faecium*, while most Gram-negative bacteria proved to be resistant at clinically relevant minimum inhibitory concentration (MIC) cutoffs (Table 1). Gladiolin was also found to be active against *C. albicans* with an MIC of 4 μg/mL (Table 1).

Table 1. MIC Values Determined for Gladiolin against *C. albicans* and a Range of Gram-Negative and Gram-Positive Bacteria

Strain	MIC (μg/mL)
Gram-negative bacteria	
Klebsiella pneumonia DSM26371	>64
Acinetobacter baumannii DSM25645	>64
Pseudomonas aeruginosa DSM29239	>64
Enterobacter cloacae DSM16690	>64
Serratia plymuthica RVH1	>64
Ralstonia mannitolilytica BCC1391	64
Burkholderia multivorans ATCC17616	64
Escherichia coli SY327	>64
Gram-positive bacteria	
Enterococcus faecium DSM25390	32
Staphylococcus aureus DSM21979	8
Bacillus subtilis DSM10	>64
Fungi	
Candida albicans SC 5314	4

Etnangien has been reported to be active against *Mycobacterium smegmatis*. We thus evaluated the *in vitro* activity of gladiolin against *M. tuberculosis* using the resazurin microtiter assay (REMA).[23] The H37Rv strain was found to be susceptible to gladiolin at a MIC of 0.4 μg/mL (Table 2, Figure S12). Gladiolin was also found to be active against several *M. tuberculosis* clinical isolates, including four that are resistant to isoniazid and one (CHUV80037024) that is resistant to both isoniazid and rifampicin (Table 2, Figure S12). Curiously, another isoniazid and rifampicin resistant isolate (CHUV80059744) was found to be resistant. While the reason for this is currently unclear, it is not due to the RpoB mutation (Ser450Leu) that confers rifampicin resistance in this strain, because the CHUV80037024 strain harbors the same mutation. The susceptibility of nonreplicating *M. tuberculosis* to gladiolin was studied using strain ss18b.[24] No activity against this strain was observed at concentrations up to 100 μg/mL, indicating that gladiolin is not active against nonreplicating mycobacterial cells (Figure S13). Control experiments with *M. tuberculosis* strain ss18b and rifampicin at 5 μg/mL showed the expected 45% inhibition of REMA turnover.

Gladiolin was found to exhibit low toxicity toward an ovarian cancer cell line (IC_{50} > 100 μM; Figure S14). Moreover, no toxicity was observed at a dose equivalent to >500 mg/kg in a *Galleria mellonella* wax moth larvae model (Figure S15).[25]

Gladiolin inhibits RNA polymerase *in vitro*. Etnangien has been shown to inhibit bacterial RNA polymerases, both *in vitro* and *in vivo*.[19] We therefore investigated the ability of gladiolin to inhibit the *M. smegmatis* RNA polymerase (RNAP)

DOI: 10.1021/jacs.7b03382
J. Am. Chem. Soc. 2017, 139, 7974−7981

Table 2. MIC Values for Gladiolin, Isoniazid and Rifampicin against Various *M. tuberculosis* Strains

Strain	Mutation	Resistance	MIC (μg/mL)		
			Gladiolin	Isoniazid	Rifampicin
H37Rv	None	None	0.4	0.04	0.001
HUG.MB.6726	*inhA*	Isoniazid	0.4	2.2	0.001
HUG.MB.3649	*inhA*	Isoniazid	1.7	0.08	0.001
CHUV80045776	*katG*	Isoniazid	1.7	2.5	0.001
HUG.MI.1020	*katG*	Isoniazid	2.3	1.3	0.001
CHUV80037024	*rpoB, inhA, katG*	Isoniazid, Rifampicin	1.7	>10	>10
CHUV80059744	*rpoB, katG*	Isoniazid, Rifampicin	>100	>10	>10

using a promoter-driven, real-time *in vitro* transcription assay.[26−28] This revealed concentration-dependent inhibition of the RNAP by gladiolin, with an IC_{50} of ~25 μg/mL (32 μM) (Figure 3). For comparison, rifampicin has an IC_{50} of 280 nM in the same assay.

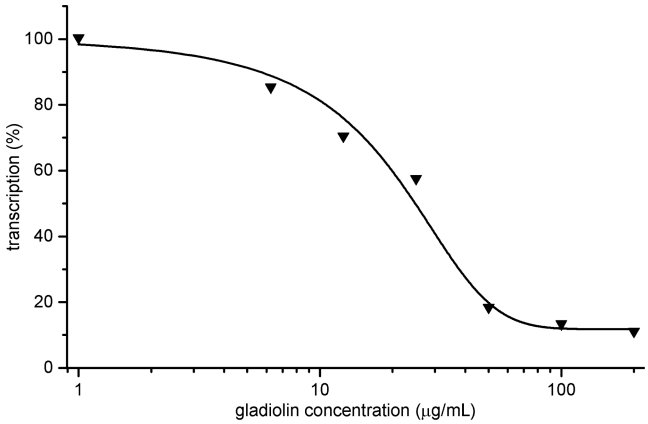

Figure 3. Concentration-dependent inhibition of the *M. smegmatis* RNA polymerase by gladiolin. The triangles represent the mean of two independent replicates which were fit to a sigmoidal dose−response function.

Sequencing and Analysis of the *B. gladioli* BCC0238 Genome. To identify the gene cluster responsible for the biosynthesis of gladiolin, we sequenced the genome of *B. gladioli* BCC0238 using SMRT sequencing technology. This approach yielded a draft genome of 8,489,985 bases that assembled into four contiguous sequences. Mapping of the resulting sequences to the complete reference genome of the rice pathogenic *B. gladioli* BSR3 strain[29] demonstrated that (i) the first contiguous sequence (4,218,485 bp) overlaps extensively with the largest chromosomal replicon of strain BSR3; (ii) the second contiguous sequence (4,046,520 bp) corresponds to the second chromosomal replicon of strain BSR3; and (iii) the third and fourth contiguous sequences (188,701 bp and 189,441 bp, respectively) show partial similarity to the *B. gladioli* BSR3 plasmid bgla_2p [NC_015377.1]. In an effort to identify and map novel genomic regions, the sequences of replicon 1 and 2 from *B. gladioli* BCC0238 were compared to the draft sequences of *B. gladioli* NBRC 13700 and 3848s-5, as well as the complete genome sequence of *B. gladioli* BSR3 (Figure S13). This analysis revealed that the sequence of replicon 1 is well conserved between isolates, whereas replicon 2 shows a considerably higher degree of sequence variability (Figure S16). Analysis of the *B. gladioli* BCC0238 genome sequence using antiSMASH v3.0[30] identified 20 and 29 putative specialized metabolite biosynthetic gene clusters on the first and second replicons, respectively (Table S4). No such clusters were found on the contiguous sequences showing similarity to the bgla_2p plasmid. A clear benefit of the long reads resulting from the SMRT sequencing was the ability to completely assemble 11 large (mean size 77,973 bp), high GC (up to 72%) and highly repetitive gene clusters encoding modular PKS and NRPS assembly lines (including one hybrid modular PKS-NRPS locus). In total, *B. gladioli* BCC0238 devotes 18.2% of the first and 25.6% of the second chromosomal replicon to specialized metabolism, based on the antiSMASH predictions.

Identification and Analysis of the Gladiolin Biosynthetic Gene Cluster. One of the putative polyketide biosynthetic gene clusters identified on the second chromosomal replicon of *B. gladioli* BCC0238 (cluster R2-11; Table S4) was postulated to direct gladiolin biosynthesis (Figure S16). This cluster harbors six large genes encoding *trans*-AT PKS subunits, designated *gbnD1-D6*, which are flanked by several genes encoding putative polyketide processing enzymes and export-related proteins (Figure S17, Table S5 and S6). To verify that this gene cluster is involved in the assembly of gladiolin, we disrupted *gbnD1* by insertional mutagenesis. UHPLC-ESI-Q-TOF-MS analysis of extracts from agar cultures confirmed that gladiolin production is abolished in the mutant (Figure 4). BLAST searches revealed a high degree of similarity between the PKS subunits involved in gladiolin and etnangien biosynthesis. Detailed analysis of the catalytic domains within the PKS subunits allowed us to propose a plausible pathway for gladiolin biosynthesis (Figure 5). In addition, sequence analysis of the KR domains within the gladiolin PKS allowed the

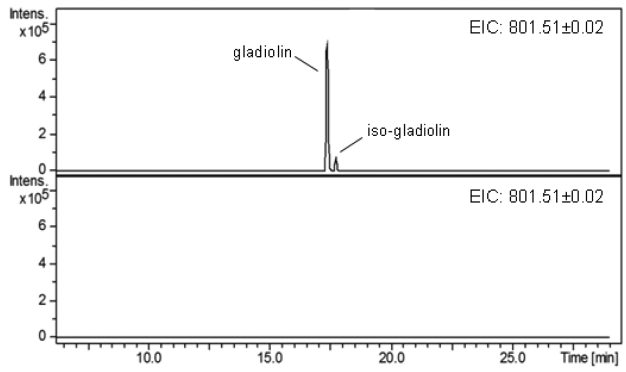

Figure 4. Insertional mutagenesis of *gbnD1* abolishes gladiolin production by *B. gladioli* BCC0238. Extracted ion chromatograms at m/z 801.51 ± 0.02, corresponding to the $[M + Na]^+$ ion of gladiolin, from LC-MS analyses of crude extracts from agar-grown cultures of *B. gladioli* BCC0238 (top) and the insertional PKS mutant *B. gladioli* BCC0238 Ω*gbnD1* (bottom).

DOI: 10.1021/jacs.7b03382
J. Am. Chem. Soc. 2017, 139, 7974−7981

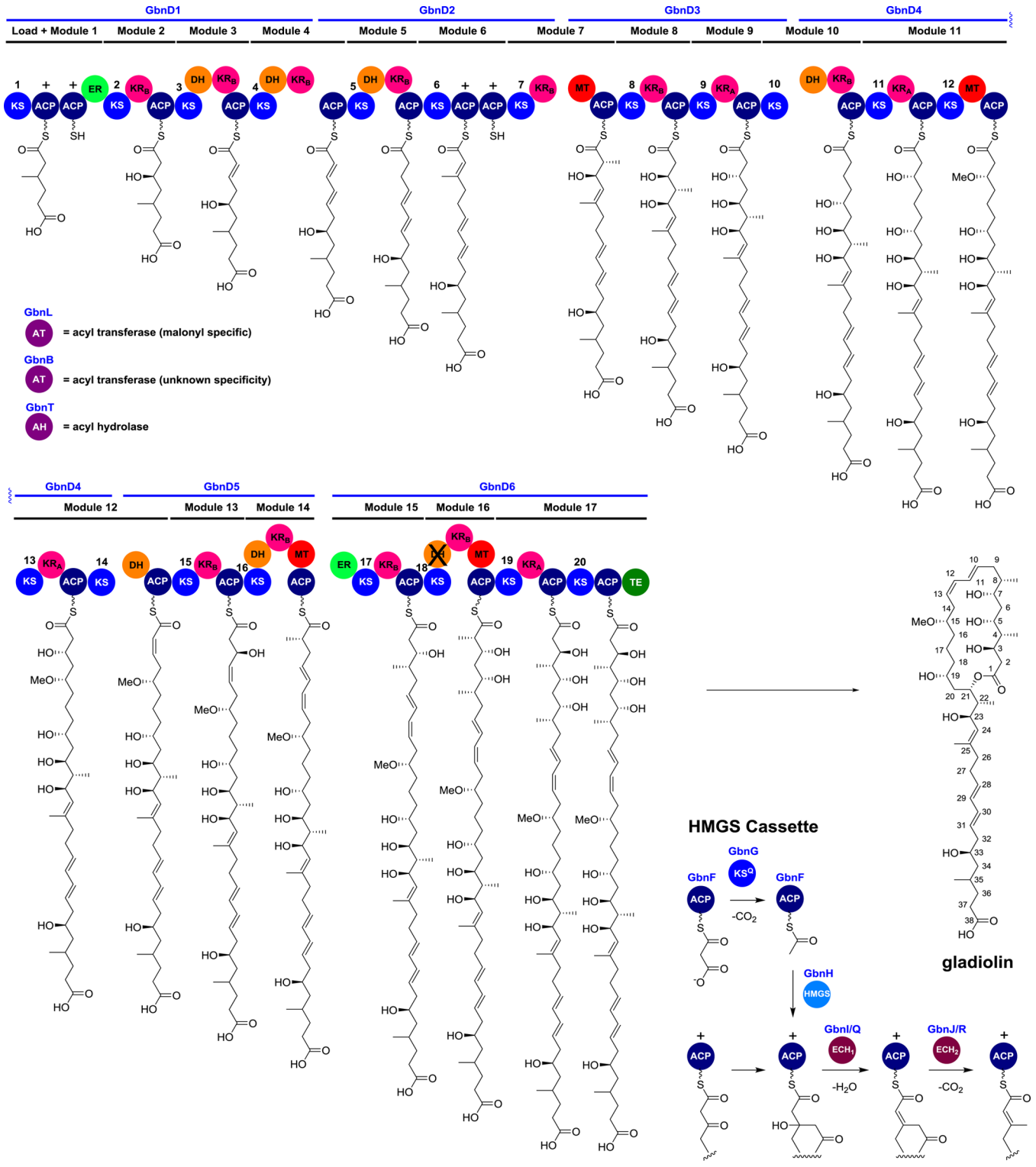

Figure 5. Proposed pathway for gladiolin biosynthesis. Domain and module organization of the gladiolin *trans*-AT PKS, showing the proposed structures of the ACP-bound thioester intermediates following α- and β-carbon processing. The configurations of the stereocenters were predicted based on sequence analysis of the KR domains. Acyl transferase/hydrolase domains acting *in trans* are shown, and their predicted specificities are indicated. Note that although the PKS harbors 20 KS domains, only 17 chain elongation reactions are required for the assembly of the gladiolin backbone. No canonical KS^0 domains were identified. However, KS12, KS14, and KS20 are hypothesized to be nonelongating KS domains. Domain abbreviations are as follows: KS, ketosynthase; KR, ketoreductase; DH, dehydratase; ER, enoyl reductase; MT, C-/O-methyltransferase; ACP, acyl carrier protein and TE, thioesterase. The predicted stereospecificity of KR domains is denoted as type A or type B in subscript. The mechanism of β-branching by the HMGS cassette is highlighted, and ACP domains in the assembly line harboring the conserved Trp residue recognized by the HMGS cassette are indicated with a "+". The putative functions of the proteins encoded by the gladiolin biosynthetic gene cluster are given in Figures S17–20 and Tables S5 and S6.

DOI: 10.1021/jacs.7b03382
J. Am. Chem. Soc. 2017, 139, 7974–7981

absolute stereochemistry of each of the stereocenters bearing a hydroxyl group to be predicted (Figure 5, Table S7).[31] These predictions are in complete agreement with the relative stereochemistry assigned to gladiolin on the basis of the NMR data (Figure 2) and allowed the configuration of the C-33 stereocenter, which could not be elucidated experimentally, to be tentatively assigned as *R* (Figure 5).

As expected for PKSs belonging to the *trans*-AT phylogenetic group, GbnD1−D6 lack AT domains. Three AT-like enzymes, GbnB, GbnN, and GbnP, are encoded by genes upstream of the PKS genes. Phylogenetic analysis of these enzymes identified GbnN as an AT with specificity for malonyl-CoA (Figure S18). In contrast, GbnB clusters with the putative etnangien biosynthetic enzyme EtnB, in a distinct clade from GbnN and GbnP. The substrate specificity of GbnB/EtnB could not be predicted from analysis of conserved sequence motifs (Figure S18).

The biosynthesis of gladiolin is proposed to be initiated by transacylation of the succinyl moiety of succinyl-CoA onto the active site Cys residue in the N-terminal ketosynthase (KS) domain of GbnD1. This hypothesis is supported by phylogenetic analyses, which place this KS in clade VI along with other KS domains that accept related PKS starter units (Figure S19).[34] Alternatively, the AT-like enzyme GbnB could catalyze transfer of the succinyl group from succinyl-CoA onto either of the ACP domains immediately downstream of the KS domain. This would require subsequent back-transfer of the succinyl unit onto the active site Cys of the KS, a phenomenon that has previously been observed in other systems *in vitro*.[35]

Following elongation of the succinyl starter unit via decarboxylative condensation with a malonyl extender unit that has been loaded onto one of the ACP domains immediately downstream of the KS domain by GbnN, a β-methyl branch is proposed to be installed by the hydroxymethylglutaryl-CoA synthase (HCS) enzyme cassette encoded by *gbnF-H* and *gbnI-J/gbnR-S*. This is the first of two such modification reactions that are proposed to take place during gladiolin assembly, the second occurring in module 6 (Figure 5). Sequence analysis of the ACP domains in modules 1 and 6 of the gladiolin PKS confirmed that they all harbor a conserved Trp residue, which has been shown to play an important role in recognition by the HCS cassette (Figure S20).[36] The product of this well-characterized β-branching process is a β-methyl-α,β-unsaturated thioester intermediate.[37]

Up until this point the intermediates in gladiolin and etnangien biosynthesis appear to be identical. Intriguingly, however, one of the three ACP domains in module 1 of the etnangien PKS is replaced with an enoyl reductase (ER) domain in the gladiolin PKS (Figure S21). The result of this domain substitution appears to be that the C−C double bond in the β-methyl-α,β-unsaturated thioester intermediate in gladiolin biosynthesis is reduced, whereas in etnangien biosynthesis the C−C double bond is preserved (Figure 5).[20] Interestingly, the gladiolin biosynthetic gene cluster encodes two sets of the enoyl-CoA hydratase (ECH) enzymes (GbnI/GbnJ and GbnR/GbnS) responsible for dehydration and decarboxylation of the 3-hydroxy-3-methylglutaryl-ACP intermediate in β-branching. In contrast, only a single set of these enzymes (EtnP/EtnQ) is encoded by the etnangien biosynthetic gene cluster (Figure S17). It is therefore tempting to speculate that the presence of the ER domain places structural constraints on the adjacent ACP domains that have necessitated the recruitment of a second set of ECH enzymes to complete formation of the β-branch in module 1 of the gladiolin PKS.

The substitution of an ACP domain with an ER domain in module 1 of GbnD1 is the only discernible difference in domain organization between gladiolin and etnangien PKSs. Thus, it seems likely that the ER domain in GbnD1 may be responsible for some of the other structural differences between gladiolin and etnangien. Arguably the most striking difference between these two compounds is the C-26/C-35 pentaene in the latter, which is substituted with a C-26/C-31 dimethylenediene in the former. The origin of the C-26/C-35 pentaene in etnangien has been attributed to iterative use of module 5, which is proposed to catalyze three successive rounds of chain elongation, ketoreduction, and dehydration.[20] The mechanism by which iterative use of module 5 is circumvented in GbnD2 is an intriguing aspect of gladiolin biosynthesis. It appears that the enoyl thioester resulting from chain elongation, ketoreduction, and dehydration by module 5 undergoes enoyl reduction, because C-26/C-27 in gladiolin is saturated. However, module 5 does not contain an ER domain. It is hypothesized that the ER domain in module 1 of the gladiolin PKS catalyzes this reaction and that this prevents transfer of the ACP-bound thioester back onto the KS domain in module 5, which is required to initiate a second round of chain elongation. A final structural difference between gladiolin and etnangien is the presence of a methyl group at C-6 in the latter. Both the etnangien and gladiolin PKSs have C-methyltransferase (MT) domains in modules 16 and 18. This is congruent with the presence of methyl groups at C-4 and C-8 in gladiolin, but is incongruent with the observation that C-4, C-6, and C-8 all bear methyl groups in etnangien. It therefore appears that the MT domain in either module 16 or module 18 of the etnangien PKS is able to catalyze C-methylation of the module 17 chain elongation intermediate.[20]

A final interesting point about gladiolin biosynthesis is that GbnD1-D6 possess 20 KS domains, but only 17 chain elongation reactions are required to assemble the polyketide chain from a succinyl-CoA starter unit and 16 malonyl-CoA extender units (Figure 5). Three of the KS domains must therefore act as transacylases, i.e. they simply transfer the polyketide chain from one ACP to another. In other *trans*-AT PKSs such transacylation reactions are typically catalyzed by KS^0 domains, which lack the His residue from the **H**GTGT motif that is required for catalysis of chain elongation.[34] However, sequence analysis revealed that all 20 of the KS domains in the gladiolin PKS harbor an intact HGTGT motif. Thus, it is difficult to predict which of them function as transacylases. Based on the structure of gladiolin and the architecture of *trans*-AT PKSs that contain KS^0 domains, we tentatively suggest that KS domains 12, 14, and 20 are likely to be nonelongating. However, experimental evidence will be required to verify this.

SUMMARY AND CONCLUSIONS

In this study, we isolated and elucidated the structure of gladiolin, a novel macrolide antibiotic produced by *B. gladioli* BCC0238. This metabolite is structurally related to etnangien, a compound of considerable interest due to its potent antimicrobial activity and its ability to efficiently inhibit nucleic acid polymerases. However, the clinical development of etnangien has been hampered by the high instability of the hexaene moiety in its C-21 side chain, which until now was thought to be essential for biological activity.[40] By virtue of its

DOI: 10.1021/jacs.7b03382
J. Am. Chem. Soc. 2017, 139, 7974−7981

shorter and more saturated C-21 side chain, gladiolin benefits from dramatically improved stability compared to etnangien, yet retains potent activity against mycobacteria via inhibition of RNA polymerase (note that although the IC_{50} for inhibition of *M. smegmatis* RNA polymerase by gladiolin is approximately 2 orders of magnitude higher than its MIC against *M. tuberculosis* H37Rv, the same is true of rifampicin, for which RNA polymerase is known to be the primary target). Moreover, gladiolin displays low toxicity and good activity against several antibiotic-resistant clinical isolates of *M. tuberculosis*. There is a pressing need to overcome multidrug resistant and extensively drug-resistant tuberculosis. Gladiolin offers potential for further development as an antibiotic to address this challenge. Using a SMRT-sequencing approach, we identified the gladiolin biosynthetic gene cluster in the genome of *B. gladioli* BCC0238. Detailed comparative analysis of the gladiolin and etnangien biosynthetic gene clusters revealed a strikingly similar domain composition in the *trans*-AT PKS assembly lines responsible for assembly of these two metabolites. The structural differences in the C-21 side chains of gladiolin and etnangien appear to be due, at least in part, to substitution of an ER domain in the gladiolin PKS with an ACP domain in the etnangien assembly line, and provide a dramatic example of evolutionary reprogramming of *trans*-AT PKS chain assembly.

EXPERIMENTAL SECTION

Gladiolin Isolation, Structure Elucidation, and Stability Analysis. For gladiolin production, *B. gladioli* BCC0238 was grown at 30 °C on solid minimal medium containing glycerol as a sole carbon source (BSM-G).[41] Following incubation for 3 days, the cells were scraped off and the agar was extracted twice using MeCN (1:1). Extracts were purified by semipreparative HPLC to give gladiolin as a white powder. Structure elucidation was achieved using a combination of UHPLC-ESI-Q-TOF-MS/MS and 1- and 2-D NMR experiments.

Susceptibility of (Non)replicating *M. tuberculosis* to Gladiolin. The susceptibility of replicating strains was determined in a 96-well plate using the resazurin reduction assay as described previously.[23,28] The susceptibility of nonreplicating *M. tuberculosis* to gladiolin was determined using the ss18b model as described previously.[24] Control experiments were conducted using rifampicin and isoniazid.

Inhibition of the Mycobacterial RNA Polymerase *in Vitro*. *M. smegmatis* RNAP holoenzyme was purified from *M. smegmatis* mc^2155 expressing a His_6-tagged RNAP β subunit (kindly provided by Dipankar Chatterjee, Indian Institute of Science) as described previously.[27,38] To measure inhibition of promoter-specific DNA-dependent RNA transcription by gladiolin, a real-time, multiple round *in vitro* transcription assay was used that employs molecular beacons.[26,27]

Genome Sequencing, Assembly, and Analysis. Genomic DNA was extracted from bacteria harvested by centrifugation from 2 mL of a fresh overnight culture of *B. gladioli* using the Maxwell 16 Tissue DNA Purification Kit and instrument (Promega) and prepared for sequencing using a DNA Template Prep Kit 2.0 (3 Kb - 10 Kb; Pacific Biosciences), following the manufacturer's instructions. The genome sequence was assembled from data obtained from two runs on a PacBio RSII sequencer. One used 3 SMRT cells, P4-C2 chemistry, and a 120m movie. The other used 3 SMRT cells, P5-C3 chemistry, and a 180m movie. 293,015 filtered subreads, with a total length of 969,973,511 bp, a mean length of 3,310bp, and a median length of 2,120bp were assembled using SMRTanalysis v2.3.0 (Pacific Biosciences). Secondary metabolite biosynthetic gene cluster predictions were made using antiSMASH v3.0,[30] and the putative gladiolin gene cluster was subjected to detailed manual annotation via comparative sequence analysis (Tables S4−S7 and Figures S13−S18).

Insertional Mutagenesis of Gladiolin Biosynthetic Gene *gbn*D1. Insertional mutagenesis was performed using the pGpΩTp suicide plasmid.[39] Primers amplifying a 446 bp region of the PKS gene *gbnD1* (Fw: 5′-ATTTCTAGAGTTGCTGATCGACGCCTATC-3′; Rev: 5′-TATGAATTCCGCCATAACCGAACGAACTC-3′) were designed. The PCR product was amplified using the Taq PCR core kit (Qiagen) and cloned, following *Xba*I and *Eco*RI digestion (NEB), into pGpΩTp. The validity of the mutagenesis construct was confirmed by sequencing. The construct was introduced into *E. coli* SY327 by electroporation and subsequently mobilized into *B. gladioli* via triparental mating.[38] Transconjugants were selected using trimethoprim (100 μg/mL) and polymyxin B (600 U/ml). A single *B. gladioli gbnD1* mutant was selected, and correct pathway disruption was confirmed by Illumina resequencing.

ASSOCIATED CONTENT

Supporting Information

The Supporting Information is available free of charge on the ACS Publications website at DOI: 10.1021/jacs.7b03382.

(PDF)

AUTHOR INFORMATION

Corresponding Authors

*MahenthiralingamE@cardiff.ac.uk

*G.L.Challis@warwick.ac.uk

ORCID

Cerith Jones: 0000-0001-6275-0235

Gregory L. Challis: 0000-0001-5976-3545

Present Address

¶Cancer Research UK Cambridge Institute, Li Ka Shing Centre, University of Cambridge, Cambridge CB2 0RE, United Kingdom.

Author Contributions

‖L.S., M.J., and J.M. contributed equally to this work.

Notes

The authors declare no competing financial interest.

ACKNOWLEDGMENTS

We thank Phillip Norville for technical assistance and Thomas Connor for advice regarding genome sequence analysis. This research was supported by grants from the BBSRC (Grant Reference BB/L021692/1) to E.M., G.L.C., and J.P, and the Welsh Government Life Sciences Bridging Fund (Grant Reference LSBF R2-004) to E.M. The Dionex 3000RS/Bruker MaXis Impact instrument used in this work was purchased with a grant to G.L.C. from the BBSRC (BB/K002341/1). J.M. was supported by a Marie Sklodowska-Curie Fellowship (Contract No. 656067).

REFERENCES

(1) Coenye, T.; Vandamme, P. *Environ. Microbiol.* **2003**, *5*, 719.

(2) Mahenthiralingam, E.; Urban, T. A.; Goldberg, J. B. *Nat. Rev. Microbiol.* **2005**, *3*, 144.

(3) O'Sullivan, L. A.; Weightman, A. J.; Jones, T. H.; Marchbank, A. M.; Tiedje, J. M.; Mahenthiralingam, E. *Environ. Microbiol.* **2007**, *9*, 1017.

(4) Suarez-Moreno, Z. R.; Caballero-Mellado, J.; Coutinho, B. G.; Mendonca-Previato, L.; James, E. K.; Venturi, V. *Microb. Ecol.* **2012**, *63*, 249.

(5) LiPuma, J. J. *Clin. Microbiol. Rev.* **2010**, *23*, 299.

(6) Parke, J. L.; Gurian-Sherman, D. *Annu. Rev. Phytopathol.* **2001**, *39*, 225.

(7) Attafuah, A.; Bradbury, J. F. *J. Appl. Bacteriol.* **1989**, *67*, 567.

DOI: 10.1021/jacs.7b03382
J. Am. Chem. Soc. 2017, 139, 7974−7981

(8) Duerkop, B. A.; Varga, J.; Chandler, J. R.; Peterson, S. B.; Herman, J. P.; Churchill, M. E. A.; Parsek, M. R.; Nierman, W. C.; Greenberg, E. P. *J. Bacteriol.* **2009**, *191*, 3909.
(9) Deng, P.; Wang, X.; Baird, S.; Showmaker, K.; Smith, L.; Peterson, D.; Lu, S. *MicrobiologyOpen* **2016**, *5*, 353.
(10) Partida-Martinez, L. P.; Groth, I.; Schmitt, I.; Richter, W.; Roth, M.; Hertweck, C. *Int. J. Syst. Evol. Microbiol.* **2007**, *57*, 2583.
(11) Moebius, N.; Ross, C.; Scherlach, K.; Rohm, B.; Roth, M.; Hertweck, C. *Chem. Biol.* **2012**, *19*, 1164.
(12) Liu, X.; Biswas, S.; Berg, M. G.; Antapli, C. M.; Xie, F.; Wang, Q.; Tang, M.-C.; Tang, G.-L.; Zhang, L.; Dreyfuss, G.; Cheng, Y.-Q. *J. Nat. Prod.* **2013**, *76*, 685.
(13) Biggins, J. B.; Gleber, C. D.; Brady, S. F. *Org. Lett.* **2011**, *13*, 1536.
(14) Eustaquio, A. S.; Janso, J. E.; Ratnayake, A. S.; Chang, L. P.; O'Donnell, C. J.; Koehn, F. E. *Planta Med.* **2015**, *81*, 860.
(15) Ishida, K.; Lincke, T.; Behnken, S.; Hertweck, C. *J. Am. Chem. Soc.* **2010**, *132*, 13966.
(16) Seyedsayamdost, M. R.; Chandler, J. R.; Blodgett, J. A. V.; Lima, P. S.; Duerkop, B. A.; Oinuma, K.-I.; Greenberg, E. P.; Clardy, J. *Org. Lett.* **2010**, *12*, 716.
(17) Mahenthiralingam, E.; Song, L.; Sass, A.; White, J.; Wilmot, C.; Marchbank, A.; Boaisha, O.; Paine, J.; Knight, D.; Challis, G. L. *Chem. Biol.* **2011**, *18*, 665.
(18) Esmaeel, Q.; Pupin, M.; Kieu, N. P.; Chataigne, G.; Bechet, M.; Deravel, J.; Krier, F.; Hofte, M.; Jacques, P.; Leclere, V. *MicrobiologyOpen* **2016**, *5*, 512.
(19) Irschik, H.; Schummer, D.; Hoefle, G.; Reichenbach, H.; Steinmetz, H.; Jansen, R. *J. Nat. Prod.* **2007**, *70*, 1060.
(20) Menche, D.; Arikan, F.; Perlova, O.; Horstmann, N.; Ahlbrecht, W.; Wenzel, S. C.; Jansen, R.; Irschik, H.; Mueller, R. *J. Am. Chem. Soc.* **2008**, *130*, 14234.
(21) Kobayashi, Y.; Tan, C. H.; Kishi, Y. *Helv. Chim. Acta* **2000**, *83*, 2562.
(22) Boucher, H. W.; Talbot, G. H.; Bradley, J. S.; Edwards, J. E.; Gilbert, D.; Rice, L. B.; Scheld, M.; Spellberg, B.; Bartlett, J. *Clin. Infect. Dis.* **2009**, *48*, 1.
(23) Martin, A.; Camacho, M.; Portaels, F.; Palomino, J. C. *Antimicrob. Agents Chemother.* **2003**, *47*, 3616.
(24) Sala, C.; Dhar, N.; Hartkoorn, R. C.; Zhang, M.; Ha, Y. H.; Schneider, P.; Cole, S. T. *Antimicrob. Agents Chemother.* **2010**, *54*, 4150.
(25) Desbois, A. P.; Coote, P. J. *Adv. Appl. Microbiol.* **2012**, *78*, 25−53.
(26) Marras, S. A. E.; Gold, B.; Kramer, F. R.; Smith, I.; Tyagi, S. *Nucleic Acids Res.* **2004**, *32*, e72.
(27) Hartkoorn, R. C.; Sala, C.; Magnet, S. J.; Chen, J. M.; Pojer, F.; Cole, S. T. *J. Bacteriol.* **2010**, *192*, 5472.
(28) Hartkoorn, R. C.; Sala, C.; Neres, J.; Pojer, F.; Magnet, S.; Mukherjee, R.; Uplekar, S.; Boy-Roettger, S.; Altmann, K.-H.; Cole, S. T. *EMBO Mol. Med.* **2012**, *4*, 1032.
(29) Seo, Y.-S.; Lim, J.; Choi, B.-S.; Kim, H.; Goo, E.; Lee, B.; Lim, J.-S.; Choi, I.-Y.; Moon, J. S.; Kim, J.; Hwang, I. *J. Bacteriol.* **2011**, *193*, 3149.
(30) Weber, T.; Blin, K.; Duddela, S.; Krug, D.; Kim, H. U.; Bruccoleri, R.; Lee, S. Y.; Fischbach, M. A.; Mueller, R.; Wohlleben, W.; Breitling, R.; Takano, E.; Medema, M. H. *Nucleic Acids Res.* **2015**, *43*, W237.
(31) Piasecki, S. K.; Zheng, J.; Axelrod, A. J.; Detelich, M. E.; Keatinge-Clay, A. T. *Proteins: Struct., Funct., Genet.* **2014**, *82*, 2067.
(32) Jensen, K.; Niederkrueger, H.; Zimmermann, K.; Vagstad, A. L.; Moldenhauer, J.; Brendel, N.; Frank, S.; Poeplau, P.; Kohlhaas, C.; Townsend, C. A.; Oldiges, M.; Hertweck, C.; Piel, J. *Chem. Biol.* **2012**, *19*, 329.
(33) Jenner, M.; Afonso, J. P.; Kohlhaas, C.; Karbaum, P.; Frank, S.; Piel, J.; Oldham, N. J. *Chem. Commun.* **2016**, *52*, 5262.
(34) Nguyen, T.; Ishida, K.; Jenke-Kodama, H.; Dittmann, E.; Gurgui, C.; Hochmuth, T.; Taudien, S.; Platzer, M.; Hertweck, C.; Piel, J. *Nat. Biotechnol.* **2008**, *26*, 225.
(35) Jenner, M.; Afonso, J. P.; Bailey, H. R.; Frank, S.; Kampa, A.; Piel, J.; Oldham, N. J. *Angew. Chem., Int. Ed.* **2015**, *54*, 1817.
(36) Haines, A. S.; Dong, X.; Song, Z.; Farmer, R.; Williams, C.; Hothersall, J.; Ploskon, E.; Wattana-amorn, P.; Stephens, E. R.; Yamada, E.; Gurney, R.; Takebayashi, Y.; Masschelein, J.; Cox, R. J.; Lavigne, R.; Willis, C. L.; Simpson, T. J.; Crosby, J.; Winn, P. J.; Thomas, C. M.; Crump, M. P. *Nat. Chem. Biol.* **2013**, *9*, 685.
(37) Calderone, C. T.; Kowtoniuk, W. E.; Kelleher, N. L.; Walsh, C. T.; Dorrestein, P. C. *Proc. Natl. Acad. Sci. U. S. A.* **2006**, *103*, 8977.
(38) Mukherjee, B.; Chatterjee, N. *Biometrics* **2008**, *64*, 685.
(39) Flannagan, R. S.; Aubert, D.; Kooi, C.; Sokol, P. A.; Valvano, M. A. *Infect. Immun.* **2007**, *75*, 1679−1689.
(40) Altendorfer, M.; Raja, A.; Sasse, F.; Irschik, H.; Menche, D. *Org. Biomol. Chem.* **2013**, *11*, 2116−2139.
(41) O'Sullivan, L. A.; Weightman, A. J.; Jones, T. H.; Marchbank, A. M.; Tiedje, J. M.; Mahenthiralingam, E. *Environ. Microbiol.* **2007**, *9*, 1017−1034.

DOI: 10.1021/jacs.7b03382
J. Am. Chem. Soc. 2017, 139, 7974−7981